

TEST OF TURBULENCE MODELS FOR THE NUMERICAL SIMULATION OF INTERNAL MIXED CONVECTION FLOWS

J.J. Costa*, S. Mergui**, J.L. Tuhault**, F. Penot**, D. Blay** and L.A. Oliveira*

* Dep. Engenharia Mecânica, Universidade de Coimbra
Largo D. Dinis
3000 Coimbra, Portugal

** Laboratoire d'Etudes Thermiques, Université de Poitiers
40, Av. du Recteur Pineau
86022 Poitiers Cedex, France

SUMMARY

In this work, the mixed convection flow generated by two non-isothermal low velocity plane jets inside a cavity with imposed wall temperatures is both experimentally and numerically investigated for one parameter configuration. Three turbulence models are used in the 2-D numerical simulation of the flow, namely the standard $k-\varepsilon$ model of Launder and Spalding with viscous sublayer wall boundary conditions and the low Reynolds number $k-\varepsilon$ models of Jones and Launder and of Launder and Sharma. Numerical and experimental results for velocity, temperature and turbulence intensity at mid-length and mid-height of the central plane are presented and comparatively analysed. The standard $k-\varepsilon$ model predicts higher temperature in the core region and velocities at the floor level than experiments. However, it performs better than the other two models which deviate from measurements in the opposite sense.

... ..

... ..

... ..

... ..

... ..

... ..

... ..

... ..

... ..

... ..

... ..

... ..

... ..

... ..

... ..

... ..

... ..

... ..

... ..

... ..

... ..

... ..

... ..

... ..

... ..

... ..

... ..

... ..

... ..

... ..

... ..

... ..

... ..

... ..

... ..

... ..

... ..

... ..

... ..

... ..

... ..

... ..

... ..

... ..

... ..

... ..

... ..

... ..

TEST OF TURBULENCE MODELS FOR THE NUMERICAL SIMULATION OF INTERNAL MIXED CONVECTION FLOWS

J.J. Costa*, S. Mergui**, J.L. Tuhaut**, F. Penot**, D. Blay** and L.A. Oliveira*

* Dep. Engenharia Mecânica, Universidade de Coimbra
Largo D. Dinis
3000 Coimbra, Portugal

** Laboratoire d'Etudes Thermiques, Université de Poitiers
40, Av. du Recteur Pineau
86022 Poitiers Cedex, France

INTRODUCTION

Flow simulation for design purposes of room-venting or air-conditioning systems is still a challenge. The two-equation $k-\varepsilon$ turbulence model of Launder and Spalding [1] has been used in most numerical studies on this subject [2–8]. This model requires the use of empirical wall functions that bridge the viscous sublayer and thereby avoid the problem of solving the flow equations up to the walls. However, the validity of this procedure is restricted to flows in which the Reynolds number is sufficiently high for the viscous effects to be unimportant or where universal wall functions are well established.

In many situations of room ventilation, velocities are small and boundary layers are neither fully turbulent and well developed nor completely laminar. Turbulence models that account for low Reynolds number and near-wall turbulence decay effects should therefore be used. Over the past two decades, several different forms of the so-called "low Reynolds number" (or "near-wall") $k-\varepsilon$ turbulence models have been published and extensively tested in a variety of boundary layer problems [9] and in the classical natural convection "window problem" [10,11]. The application of such models to mixed convection low velocity flows, like those occurring in room ventilation, has however been scarce. In [12], the computation of airflow in a displacement ventilation system was performed using a low- Re $k-\varepsilon$ model of turbulence with modified wall boundary conditions for the turbulence variables. In a very recent paper [13], the same procedure was adopted to the three-dimensional calculations of indoor airflow and heat transfer generated by a mixing ventilation system.

In the present work, the two-dimensional recirculating flow generated by two non-isothermal low velocity jets inside a compartment is both experimentally and numerically investigated. The physical model used can be classified as a mixing flow ventilation system,

where fresh air is horizontally injected near the ceiling. Heat input is simulated by a vertical warm air jet at the floor, thus avoiding the need to account for radiative exchanges. The case studied refers to warm jet discharge Reynolds and Froude numbers of 756 and 5, respectively, cold to warm jet discharge velocity ratio of 0.826 and a global Archimedes number of 0.003, with the walls at a constant and uniform temperature equal to that of the supply (cold) air. Velocity and temperature measurements are presented for the symmetry plane. Experimental data are then used as a reference to assess the accuracy of the numerical solutions obtained with two low-Reynolds-number $k-\epsilon$ turbulence models [14,15] and the original formulation of the $k-\epsilon$ model [1], with a viscous sublayer treatment for wall boundary conditions. This validation analysis will lead to the selection of the most suitable numerical method to be used in future parametric studies. Globally, experimental results are better approached by the standard $k-\epsilon$ model which predicts slightly higher velocities at the floor level and temperatures in the core region, conversely to the other two models.

TEST APPARATUS AND EXPERIMENTAL CONDITIONS

Experimental Model

The test apparatus was designed so as to generate a two-dimensional flow, in order to ensure that experiments and corresponding calculations were not too cumbersome.

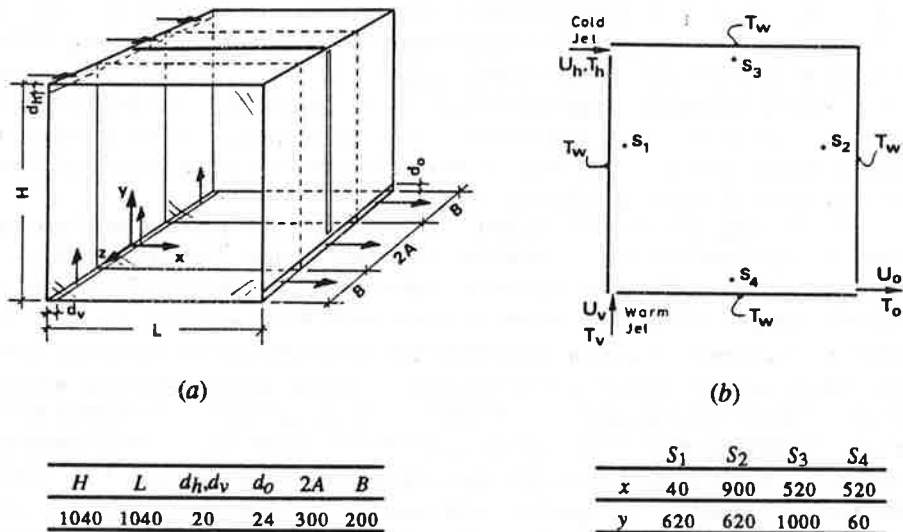


Fig. 1. (a) Configuration and dimensions (in mm) of the experimental model and the coordinate system adopted. (b) Sketch of the flow geometry in the test cavity cross section and different locations selected for monitoring purposes.

Experiments were performed on a laboratory model composed of a 1040 mm x 1040 mm x 70 mm cavity equipped with two inlet slots (20 mm wide) and one outlet slot (24 mm wide), as sketched in Fig. 1 (a). This cavity was divided into three identical smaller ones, the central working cavity (300 mm wide) where measurements were performed and two side cavities (200 mm wide each) where similar flow and temperature fields as in the working cavity were reproduced. This design made it possible to obtain a fairly good two-dimensional temperature field in the central cavity by significantly reducing end effects.

Walls of dimensions $L \times H$ (parallel to the xoy plane) were made of transparent 2 mm plexiglass, in order to allow velocity measurements by laser-Döppler anemometry (LDA). The two walls separating the test section from the guard cavities were considered to be adiabatic. Each of the four active walls ($x/L = 0$ and 1 , $y/H = 0$ and 1) was made of flat aluminium heat exchangers, maintained at a constant and uniform temperature by the use of temperature controlled water. The water flow rate was oversized to ensure that no significant temperature gradient could prevail anywhere on the wall surface. Under these conditions, the imposed wall surface temperature could be chosen between 10 °C and 50 °C with a precision of 0.25 °C. The inner surfaces of the active walls were carefully polished, so as to minimize radiation exchange between them. A 15 mm wide slot was provided at the top wall ($y/H = 1$) for the passage of a temperature probe and its displacement in a xoy plane. At the $x/L = 1$ vertical wall, a narrow glass window allowed the introduction of a light sheet for flow visualization in the test cavity.

There were two independent air circuits. They respectively fed the horizontal (cold) jet and the vertical (warm) jet. The air flow passed through a porous medium and a honeycombed structure in order to provide uniform velocity all along each slot. The air was cooled down or warmed up using a water-air heat exchanger. Water temperature was controlled by a cryothermostat with a precision of 0.25 °C. This device allowed to impose the air inlet temperature and velocity within the respective ranges:

- 10 °C to 40 °C for the horizontal cold jet and 20 °C to 70 °C for the vertical warm jet;
- 0.1 m/s up to 0.6 m/s for both jets.

The velocity measurements were performed with of a two-component laser-Döppler anemometry system in a forward scattering configuration which allowed to measure simultaneously both the horizontal and the vertical time-mean velocity components projected on a xoy plane and the respective mean square fluctuations. Temperature was measured with a 25 μ m thermocouple which could sweep a xoy plane in the central cavity.

Preliminary measurements were made on the free jet issuing from each slot (before fitting up in the cavity) to check the 2-D behaviour of the air outflow. The two-dimensionality of the mean axial velocity and temperature profiles measured along the slot centre line was within ± 5 and 1 percent of the respective mean values.

The flow configuration considered in the present study is schematically represented in Fig. 1 (b), with the nomenclature used for wall and air inlet conditions.

Scaling Parameters

Such mixed convection flows are physically interesting for the balance between inertial and buoyancy forces. Depending on the relative importance of these two forces, the

flow structure can vary significantly.

In the case of a single buoyant wall jet in a semi-infinite medium at uniform temperature, the problem is governed by three non-dimensional parameters: the jet Reynolds number, Re , the jet Froude number, Fr , and the dimensionless temperature Θ_w of the wall, if this one is not adiabatic.

Similarly, the present problem of two buoyant wall jets in a confined medium with imposed temperature walls is completely defined by the following parameters:

- vertical, warm jet Reynolds number, $Re_v = U_v D / \nu$
- vertical jet Froude number, $Fr_v = U_v / \sqrt{g \beta D (T_v - T_h)}$
- dimensionless temperature of the wall surfaces, $\Theta_w = (T_w - T_h) / (T_v - T_h)$
- horizontal to vertical jet discharge velocity ratio, U_h / U_v , and
- horizontal to vertical jet discharge temperature ratio, Θ_h / Θ_v ,

where $D (= d_h = d_v)$ is the jet slot width. The dimensionless temperature is defined as $\Theta = (T - T_h) / (T_v - T_h)$, the chosen characteristic excess temperature being the difference between the vertical (warm) and the horizontal (cold) jet discharge temperatures, T_v and T_h , respectively. Likewise, the vertical jet discharge velocity, U_v , was used as a reference to non-dimensionalize the velocity field results. A global Archimedes number is additionally defined, Ar ($Ar = g \beta D (T_o - T_h) / U_o^2$, where T_o and U_o are the mean outlet temperature and velocity, respectively), which represents the ratio between buoyancy and inertia forces in the cavity.

Air Inlet Conditions

Velocity and temperature measurements were made to characterize the air flow at the slot exits.

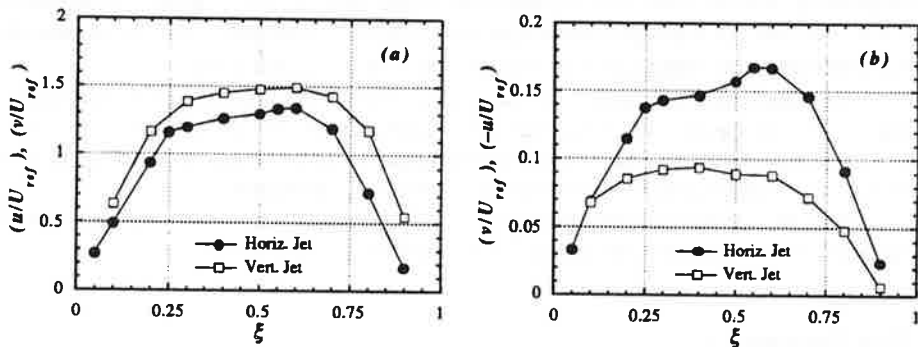


Fig. 2. (see next page for caption).

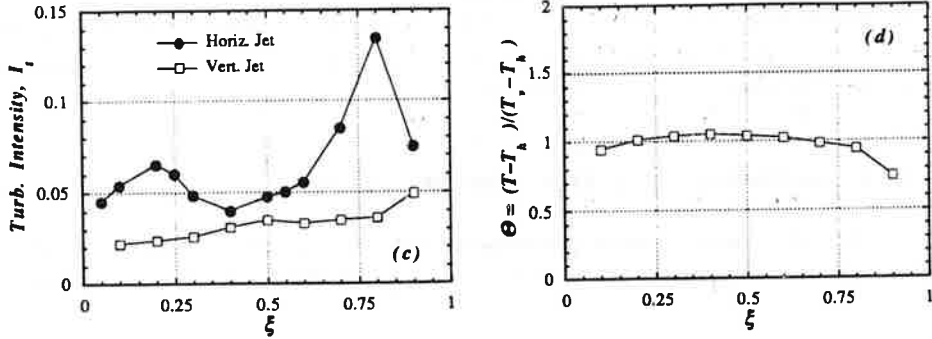


Fig. 2. Transverse profiles measured for both jets at the symmetry plane $z/A = 0$: (a) axial mean velocity component, (b) normal mean velocity component and (c) turbulence intensity at each jet exit; (d) temperature at the vertical (warm) jet slot exit. $U_{ref} = U_v = 0.59$ m/s; $T_v = 35$ °C, $T_h = 14$ °C.

The transverse profiles obtained at the central plane ($z/A = 0$) are shown in Fig. 2, where ξ is defined as $(H - y)/D$ for the horizontal jet and as x/D for the vertical jet; u and v represent the time-mean velocity components along the x and y directions, respectively, and the turbulence intensity is defined as $I_t = [(\overline{u'^2} + \overline{v'^2})/2]^{1/2} / U_{ref}$, u' and v' being the instantaneous velocity fluctuations. In both jets, the normal mean velocity component is directed towards the corresponding adjacent wall.

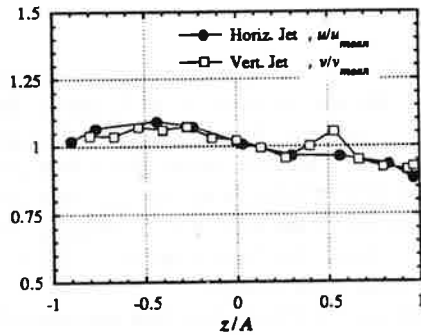


Fig. 3. Axial mean velocity measured along the exit slot centre line of each jet, normalized by the respective average value along the spanwise direction: $u_{mean} = 0.74$ m/s; $v_{mean} = 0.82$ m/s.

Some asymmetries were found in the spanwise axial mean velocity profiles measured along the centre line of each jet exit, which are plotted in Fig. 3. However, the two-dimensionality of both jets exit flow, over the central 90% of their spanwise width, lies

within ± 10 percent of the respective axial mean velocity average values, u_{mean} and v_{mean} .

The resulting wall and inlet air average conditions for the case studied in the present work are expressed in terms of the above defined dimensionless parameters: $Re_v = 756$, $Fr_v = 5$, $U_h / U_v = 0.826$. In the present condition, $\Theta_w = (\Theta_h / \Theta_v) = 0$ is used for validation purposes. This may not be the case of future parametric studies.

Two-Dimensionality of the Flow inside the Cavity

In order to evaluate the two-dimensional character of the recirculating flow inside the test cavity, velocity profiles were measured in the spanwise direction at several locations.

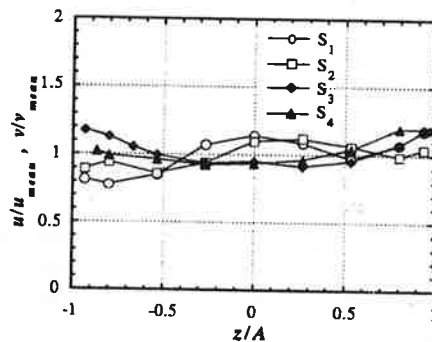


Fig. 4. Profiles of the streamwise velocity component measured along z direction at stations S_1 , S_2 , S_3 and S_4 (see Fig. 1 (b)) and normalized by the respective mean value, u_{mean} or v_{mean} .

The streamwise velocity profiles registered along the spanwise direction at levels S_1 , S_2 , S_3 and S_4 (see Fig. 1 (b)), are plotted in Fig. 4. At S_1 and S_2 , the flow is nearly vertical, ascending and descending, respectively. In both cases, the flow turns out to be stronger at the central part of the cavity width, the velocity at $z/A = 0$ being in excess of 14.1 and 9.8 percent of the corresponding profile mean value (v_{mean}), respectively at S_1 and S_2 . On the contrary, at stations S_3 and S_4 where the flow is predominantly horizontal, the streamwise velocity values at the central plane $z/A = 0$ are, respectively, 5.2 and 6.5 percent lower than the corresponding profile average value (u_{mean}).

The two-dimensionality of the temperature field was tested (by rotating the L-shaped support of the temperature probe) at the horizontal plane $y/H = 0.19$ and showed to be within 1% of the characteristic temperature difference, in the central 200 mm of the working cavity width.

THEORETICAL TREATMENT

The flow geometry considered for the theoretical study is shown in Fig. 1 (b). To simplify the problem, the flow was considered to be two-dimensional, incompressible, steady-state in mean and the Boussinesq approximation [16] was assumed for the fluid physical properties.

Mean Flow Equations

The time-averaged equations for the conservation of mass, momentum and energy can be expressed in tensor notation as

$$\frac{\partial u_i}{\partial x_i} = 0 \quad (1)$$

$$\frac{\partial}{\partial x_j} (\rho u_j u_i) = -\frac{\partial p}{\partial x_i} + \frac{\partial}{\partial x_j} \left[\mu \left(\frac{\partial u_i}{\partial x_j} + \frac{\partial u_j}{\partial x_i} \right) \right] + \rho g_i \beta (T - T_{ref}) + \frac{\partial}{\partial x_j} (-\rho \overline{u_i u_j}) \quad (2)$$

$$\frac{\partial}{\partial x_j} (\rho u_j T) = \frac{\partial}{\partial x_j} \left(\frac{\mu}{Pr} \frac{\partial T}{\partial x_j} \right) + \frac{\partial}{\partial x_j} (-\rho \overline{u_j T'}) \quad (3)$$

where u_i and u'_i are the mean and the fluctuating velocity components in the x_i direction, ρ is density, μ is the laminar viscosity, p is pressure, β is the volumetric thermal expansion coefficient, g_i is the gravitational acceleration in the i th direction and T_{ref} is some reference temperature taken here as $(T_v + T_h)/2$. The turbulence correlations $-\rho \overline{u_i u_j}$ and $-\rho \overline{u_j T'}$ stand for the time-averaged Reynolds stresses and turbulent heat fluxes, respectively, which must be modeled to close the above set of equations.

Turbulence Models

In the present study, calculations have been made with three distinct k - ϵ turbulence models, namely the original high Reynolds number formulation [1] — denoted here as standard k - ϵ model — and two versions of its extension to account for low Reynolds number and near-wall effects, which are the models of Jones and Launder (JL) [14] and of Launder and Sharma (LS) [15]. The generalized Boussinesq eddy viscosity concept is commonly adopted, expressing the turbulent stresses — by analogy with the laminar viscous stresses — as

$$-\rho \overline{u_i u_j} = \mu_t \left(\frac{\partial u_i}{\partial x_j} + \frac{\partial u_j}{\partial x_i} \right) - \frac{2}{3} \rho k \delta_{ij} \quad (4)$$

where δ_{ij} is the Kronecker delta ($\delta_{ij} = 1$ for $i = j$; $\delta_{ij} = 0$ for $i \neq j$) and μ_t is the turbulent viscosity that may be related to the turbulent kinetic energy, $k (= \overline{u'_i u'_i} / 2)$, and its dissipation rate, ϵ , by dimensional analysis:

$$\mu_t = C_\mu f_\mu \rho \frac{k^2}{\epsilon} \tag{5}$$

In an analogous way, the turbulent heat fluxes in Eq. (3) are modelled as:

$$-\overline{\rho u_j T} = \frac{\mu_t}{Pr_t} \frac{\partial T}{\partial x_j} \tag{6}$$

where Pr_t is the turbulent Prandtl number. The differential equations for k and ϵ are

$$\frac{\partial}{\partial x_j} (\rho u_j k) = \frac{\partial}{\partial x_j} \left[\left(\mu + \frac{\mu_t}{\sigma_k} \right) \frac{\partial k}{\partial x_j} \right] + P_k + G_k - \rho \epsilon + D_k \tag{7}$$

$$\begin{aligned} \frac{\partial}{\partial x_j} (\rho u_j \epsilon) = \frac{\partial}{\partial x_j} \left[\left(\mu + \frac{\mu_t}{\sigma_\epsilon} \right) \frac{\partial \epsilon}{\partial x_j} \right] + C_1 f_1 \frac{\epsilon}{k} P_k + \\ + C_1 C_3 \frac{\epsilon}{k} G_k - C_2 f_2 \rho \frac{\epsilon^2}{k} + E_\epsilon \end{aligned} \tag{8}$$

where

$$P_k = \mu_t \left(\frac{\partial u_i}{\partial x_j} + \frac{\partial u_j}{\partial x_i} \right) \frac{\partial u_i}{\partial x_j} \tag{9}$$

is the rate of production of k due to the interaction of turbulent stresses with mean velocity gradients and

$$G_k = -g_j \beta \frac{\mu_t}{Pr_t} \frac{\partial T}{\partial x_j} \tag{10}$$

is the production or destruction of the turbulent energy by thermal stratification effects.

Table I. Extra-terms and damping functions of the turbulence models. $Re_t = \rho k^2 / \mu \epsilon$ is called the turbulent Reynolds number.

Model	f_μ	f_1	f_2	D_k	E_ϵ
Standard $k-\epsilon$ [1]	1	1	1	0	0
IL [14]	$\exp\left(\frac{-2.5}{1+Re_t/50}\right)$	1	$1-0.3 \exp(-Re_t^2)$	$-2\mu \left(\frac{\partial \sqrt{k}}{\partial x_j}\right)^2$	$-2\frac{\mu \mu_t}{\rho} \left(\frac{\partial^2 u_i}{\partial x_j \partial x_k}\right)^2$
LS [15]	$\exp\left[\frac{-3.4}{(1+Re_t/50)^2}\right]$	1	$1-0.3 \exp(-Re_t^2)$	$-2\mu \left(\frac{\partial \sqrt{k}}{\partial x_j}\right)^2$	$-2\frac{\mu \mu_t}{\rho} \left(\frac{\partial^2 u_i}{\partial x_j \partial x_k}\right)^2$

The extra-terms D_k and E_ε , as well as the damping functions f_μ, f_1 and f_2 , are included to better represent the near-wall behaviour and are listed in Table I. The following empirical constant values are common to the three turbulence models used: $C_\mu = 0.09$, $C_1 = 1.44$, $C_2 = 1.92$, $C_3 = 1.0$, $\sigma_k = 1.0$, $\sigma_\varepsilon = 1.3$ and $Pr_t = 0.9$.

Boundary Conditions

The above set of transport equations was solved with the following boundary conditions (see Fig. 1 (b)):

(i) Jet inlet conditions:

$u, v, T =$ measured profiles (Figs. 2 (a), (b) and (d));

$k_{in} = \frac{3}{2} I_{in}^2 U_{ref}^2$ and $\varepsilon_{in} = k_{in}^{3/2}/D$, where I_{in} is the turbulence intensity measured

for each jet (Fig. 2 (c)).

(ii) Exit conditions:

$$\frac{\partial v}{\partial x} = \frac{\partial T}{\partial x} = \frac{\partial k}{\partial x} = \frac{\partial \varepsilon}{\partial x} = 0$$

and a correction was iteratively made to u at the exit section in order to ensure overall mass conservation.

(iii) Walls:

$$u = v = 0, T = T_w.$$

$k = \varepsilon = 0$ in the models of JL and LS. Due to grid refinement, the first inner grid point in the present calculations lies within the viscous sublayer region along each wall. Therefore, only k and ε are treated differently in the standard $k-\varepsilon$ model: ε is specified ($\varepsilon = C_\mu^{3/4} k^{3/2} / \kappa x_n$, where κ is the von Karman constant and x_n is the distance from the wall) and terms P_k and $-\rho\varepsilon$ in the k equation are modified at the first inner grid point, to account for the usual Couette flow hypothesis (near-wall linear variation of the tangential velocity component). This procedure is similar to the one adopted in [12].

Numerical Solution Procedure

The partial differential equations were discretized using the finite volume method described in [17]. The approximation of the convective fluxes applied at each control volume face was performed using the hybrid central/upwind difference scheme. The velocities and pressures were calculated by the SIMPLEC algorithm with the modifications recommended in [18]. The tri-diagonal matrix algorithm (TDMA) was applied for solving the discretized equations. Although negligible differences were observed in the solutions with respect to a grid of 52x52, the calculations were performed on a 62x62 one with a ratio of 1.2 between every two consecutive grid spaces, the first point being 0.18 mm distant from the wall. Convergence was attained when the normalized sum of the absolute residuals for the three equations of momentum and energy conservation were less than 2.5×10^{-5} .

RESULTS AND DISCUSSION

The velocity and temperature measurements were carried out along the central plane ($z/A = 0$) at several hundreds of points distributed by 17×20 and 11×10 (rows \times columns) cartesian meshes, respectively.

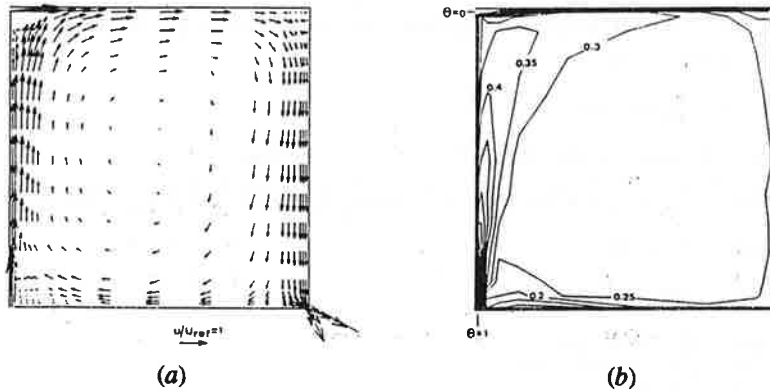


Fig. 5. Velocity vectors (a) and isotherms (b) obtained from measurements at the symmetry plane ($z/A = 0$).

The corresponding results are shown in Figs. 5 (a) and (b) in the form of mean local velocity vectors and isothermal lines, respectively. The flow pattern is dominated by the inertial momentum of both jets and thereby characterized by a single clockwise vortex.

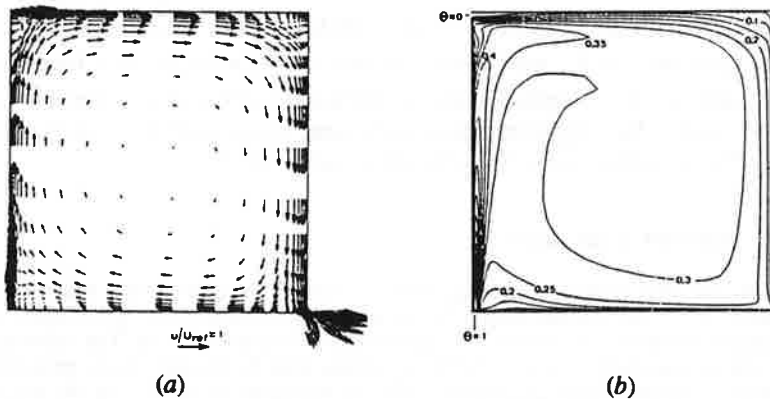


Fig. 6. Predicted (a) velocity vectors and (b) isotherms obtained with the standard $k-\epsilon$ turbulence model.

In spite of the adverse temperature gradients along the left vertical wall ($x/L = 0$) and at the horizontal cold jet, no distortion effects due to negative buoyancy are patent. The measured temperature field of Fig. 5 (b) shows that the core region of the cavity is practically isothermal with values of Θ between 0.25 and 0.3 and that stratification is restricted to the proximity of the horizontal walls and the warm jet.

The calculated velocity and temperature fields using the standard high Reynolds number $k-\varepsilon$ model are represented in Fig. 6 and show a reasonable qualitative agreement with measurements. Although slightly overestimated, the predicted temperature distribution within the core region is rather uniform, in agreement with measurements. While in the calculated temperature field the presence of the horizontal jet is well evidenced by the smoother temperature gradients close to $y/H = 1$, thereby acting in a way as an insulation between the core and the ceiling, a similar effect does not appear in the measurements. This is in part due to the lack of two-dimensionality of the flow in that region, by which the horizontal (cold) jet is weakened in the symmetry plane $z/A = 0$ (see profile S_3 in Fig. 4) where the measurements in Fig. 5 were performed. On the other hand, the turbulent mixing in that region of unstable stratification may not be properly represented by the turbulence model. In fact, the constant C_3 multiplying the buoyancy term in the ε equation has not a universal value. The assumption $C_3 = 1$ used in the present calculations is recommended for vertical buoyant shear layers and may not be satisfactory for the horizontal layer of the cold jet, where it should probably take values close to zero [19].

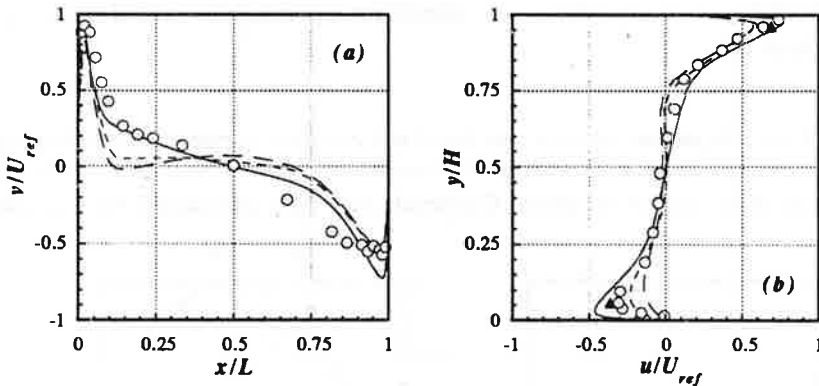


Fig. 7. Measured and calculated (a) horizontal and (b) vertical profiles of the mean velocity streamwise component at $y/H = 0.48$ and $x/L = 0.5$, respectively. \circ Experiments; — standard $k-\varepsilon$ model; - - - model of JL; - · - model of LS. \blacktriangle are the normalized mean values u_{mean}/U_{ref} of profiles S_3 and S_4 in Fig. 4.

The global differences between measurements and the numerical predictions given by the three tested turbulence models can be analysed through the wall-to-wall profiles presented in Figs. 7, 8 and 9. The standard $k-\varepsilon$ model approaches the measured mean vertical velocity at $y/H = 0.48$ (Fig. 7 (a)) better than any of the two models of JL and LS. This is also the case for the vertical profiles of horizontal velocity (Fig. 7 (b)) taken at $x/L =$

0.5, particularly if the tendency of a two-dimensional local correction of the measured values (symbol \blacktriangle in the figure) is taken into account. At the floor level, the corrected experimental value is exceeded in 10 percent of U_{ref} by the maximum horizontal velocity as predicted by the standard $k-\epsilon$ model, while it is underpredicted in 22 and 13 percent by the JL and LS models, respectively.

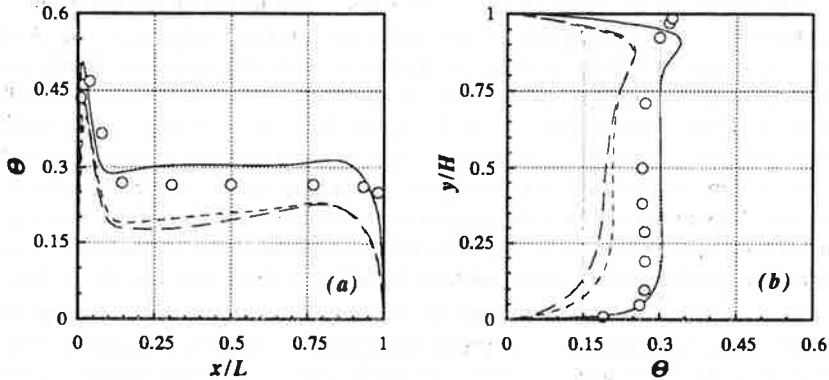


Fig. 8. (a) Horizontal and (b) vertical temperature distribution at $y/H = 0.48$ and $x/L = 0.5$, respectively. \circ Experiments; — standard $k-\epsilon$ model; --- model of JL; - · - model of LS.

From the comparison between calculated and measured temperature levels of the cavity core (Figs. 8 (a) and (b)), it can be concluded that the wall heat losses are underpredicted by the standard $k-\epsilon$ model. Conversely, they are overestimated by the JL and

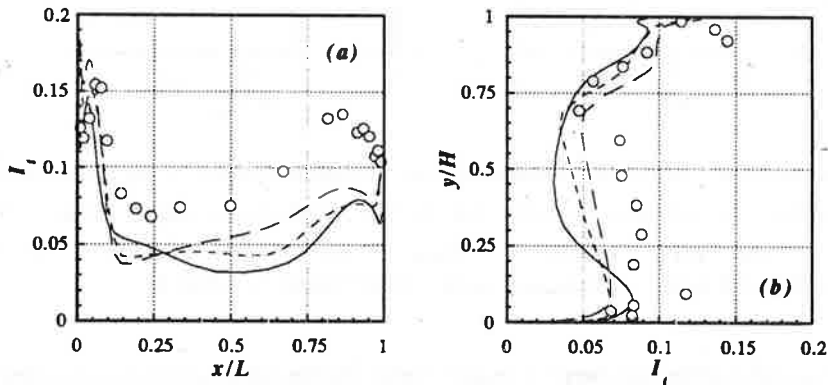


Fig. 9. Measured and predicted turbulence intensity distributions (a) at $y/H = 0.48$ and (b) $x/L = 0.5$. \circ Experiments; — standard $k-\epsilon$ model; --- model of JL; - · - model of LS.

LS models which calculate lower temperatures than the experimental values all over the domain. Having in mind that the wall heat fluxes are evaluated by expressions like the diffusive term $(\mu/Pr + \mu_t/Pr_t)(\partial T/\partial x_j)$, it may be expected that the use of higher values of the turbulent Prandtl number and/or a more efficient damping of turbulence in the near-wall regions would improve the performance of both low- Re turbulence models. It should be noted that the only difference between the JL and LS models is the expression of f_μ which provides higher near-wall damping of turbulent viscosity in the latter, thereby leading to a slightly better representation of wall heat fluxes and, consequently, of the temperature field.

The profiles plotted in Figs. 9 (a) and (b) represent the turbulence intensity which is defined as $I_t = (2/3 k)^{1/2}/U_{ref}$ when evaluated from the numerical results. The I_t level in the core region is underestimated by all three turbulence models. Particular attention should be given to the profiles at $x/L \rightarrow 0$ in Fig. 9 (a), once the left wall is responsible for 60 to 67 percent — depending on the model used — of the overall predicted heat losses. It is seen that the turbulence intensity as predicted by the models of JL and LS at $x/L = 10^{-2}$ is about 5 percent in excess of the experimental value, unlike the one given by the standard $k-\epsilon$ model ($\sim 1\%$ lower). This is in agreement with the above analysis on the influence of wall turbulence damping upon the wall heat flux evaluation.

CONCLUDING REMARKS

The mixed convection flow generated by two non-isothermal low velocity plane jets inside a cavity with imposed wall temperatures was both experimentally and numerically investigated. Measured values for the inlet air conditions were reported and used as boundary conditions for the mathematical model. The experimental data at the symmetry plane were taken as a reference for the test of three turbulence models in the 2-D numerical simulation of the flow.

Even though special care was taken to ensure the two-dimensionality of both dynamic and thermal boundary conditions, it was seen that slight 3-D effects may easily arise as the flow develops within the cavity. The global spanwise invariance should thus be a point of careful improvement for future experiments.

Calculations were performed with a non-uniform grid finely concentrated close to the walls, which required a viscous sublayer treatment of the wall boundary conditions in the standard high- Re $k-\epsilon$ turbulence model. Low Reynolds number turbulence models of Jones and Launder [14] and of Launder and Sharma [15] were parallelly tested and showed to overestimate the wall heat fluxes, unlike the standard $k-\epsilon$ model which predicts higher — yet closer — values of the core temperature level than experiments. Although the velocity field has been better reproduced by the latter model, further work should be dedicated to study the performance of more recent low- Re turbulence models in the numerical simulation of such mixed convection low velocity flows. In any case, particular attention must be given to the influence of the turbulent Prandtl number and of the damping of near-wall turbulence on the wall heat fluxes. Alternative definitions of the buoyancy-related terms and empirical constants in the turbulence equations should also be considered, so as to reproduce the

thermal instability effects in both vertical and horizontal layers in an equally satisfactory way.

ACKNOWLEDGEMENTS

The experiments reported in the present work were conducted in the *Laboratoire d'Etudes Thermiques* of the University of Poitiers and were supported by the Department of Electricity Application of *Electricité de France*. The cooperation between the Universities of Coimbra and Poitiers was supported by the corresponding Portuguese and French Governments, through the *Instituto Nacional de Investigação Científica* and the *Ambassade de France au Portugal*.

REFERENCES

- [1] Launder, B. E. and Spalding, D. B. "The Numerical Computation of Turbulent Flows". *Comp. Meth. Appl. Mech. Engng.* 1974, 3, pp. 269-289.
- [2] Restivo, A. "Turbulent Flow in Ventilated Rooms", 1979, Ph. D. Thesis, Dept. Mech. Engng., Imperial College of Science and Technology, London.
- [3] Nielsen, P. V., Restivo, A. and Whitelaw, J. H. "Buoyancy-Affected Flows in Ventilated Rooms", *Num. Heat Transfer*, 1979, 2, pp. 115-127.
- [4] Gosman, A. D., Nielsen, P. V., Restivo, A. and Whitelaw, J. H. "The Flow Properties of Rooms with Small Ventilation Openings", *J. Fluids Engng.*, 1980, 102, pp.316-323.
- [5] Whittle, G. E. "Computation of Air Movement and Convective Heat Transfer within Buildings". *Int. J. Ambient Energy*, 1986, 7, 3, pp. 151-164.
- [6] Awbi, H. B. "Application of Computational Fluid Dynamics in Room Ventilation". *Building and Environment*, 1989, 24, 1, pp. 73-84.
- [7] Murakami, S. and Kato, S. "Numerical and Experimental Study on Room Airflow—3-D Predictions using the $k-\epsilon$ Turbulence Model". *Building and Environment*, 1989, 24, 1, pp. 85-97.
- [8] Davidson, L. "Ventilation by Displacement in a Three-Dimensional Room: a Numerical Study". *Building and Environment*, 1989, 24, 4, p. 363.
- [9] Patel, V. C., Rodi, W. and Scheuerer, G. "Turbulence Models for Near-Wall and Low Reynolds Number Flows: A Review". *AIAA J.*, 1984, 25, pp.

1308-1319.

- [10] Davidson, L. "Calculation of the Turbulent Buoyancy-Driven Flow in a Rectangular Cavity using an Efficient Solver and Two Different Low Reynolds Number $k-\epsilon$ Turbulence Models". Num. Heat Transfer, A, 1990, 18, pp. 129-147.
- [11] Henkes, R. A. "Natural-Convection Boundary Layers". 1990, Ph.D. Thesis, Faculty of Applied Physics, Delft University of Technology, The Netherlands.
- [12] Chen, Q., Suter, P. and Moser, A. "Influence of Air Supply Parameters on Indoor Air Diffusion". Building and Environment, 1991, 26, 4, pp. 417-431.
- [13] Chen, Q. and Jiang, Z. "Air Supply Method and Indoor Environment". Indoor Environment, 1992, 1, pp. 88-102.
- [14] Jones, W. P. and Launder, B. E. "The Calculation of Low-Reynolds Number Phenomena with a Two-Equation Model of Turbulence". Int. J. Heat Mass Transfer, 1973, 16, pp. 1119-1130.
- [15] Launder, B. E. and Sharma, B. I. "Application of the Energy-Dissipation Model of Turbulence to the Calculation of Flow near a Spinning Disk". Lett. Heat Mass Transfer, 1974, 1, pp. 131-138.
- [16] Gray, D. D. and Giorgini, A. "The Validity of the Boussinesq Approximation for Liquids and Gases". Int. J. Heat and Mass Transfer, 1976, 19, pp. 545-551.
- [17] Patankar, S. V. "Numerical Heat Transfer and Heat Flow". McGraw-Hill, New York, 1980.
- [18] Van Doormaal, J. P. and Raithby, G. D. "Enhancements of the SIMPLE Method for Predicting Incompressible Fluid Flows". Num. Heat Transfer, 1984, 7, pp.147-163.
- [19] Rodi, W. "Turbulence Models and their Application in Hydraulics — A State of the Art Review". 1980, University of Karlsruhe, Germany, p. 30.

